

# Behaviors of cylindrical rock specimen under dynamic load

Shiro Kubota<sup>\*†</sup>, Yuji Ogata<sup>\*</sup>, Yuji Wada<sup>\*</sup>, Ganda Simangunsong<sup>\*</sup>,  
Hideki Shimada<sup>\*\*</sup>, and Kikuo Matsui<sup>\*\*</sup>

<sup>\*</sup>Research Center for Explosion Safety, National Institute of Advanced Industrial Science and Technology,  
16-1 Onogawa, Tsukuba, Ibaraki 305-8569, JAPAN

<sup>†</sup> Corresponding address: kubota.46@aist.go.jp

<sup>\*\*</sup>Department of Earth Resources Engineering, Faculty of Engineering, Kyushu University,  
6-10-1 Hakozaki, Higashi-ku, Fukuoka 812-8581, JAPAN

Received: April 20, 2006 Accepted: May 25, 2006

## Abstract

Behaviors of cylindrical rock specimen under dynamic load have been investigated by proposed test. The Hopkinson's effect at free end of specimen has been employed in this dynamic test. The PMMA pipe filled with water is arranged between the explosive and cylindrical rock specimen, and the length of the pipe is varied to adjust the strength of dynamic loading. A series of the dynamic test were carried out for Kimachi sandstone. The propagation processes of the tensile stress in the specimen were reproduced by the velocity profiles. From the distributions of the tensile stress near the free end, the relationships of the region or position of fracture surface and the stress distribution have been clearly understood.

**Keywords:** Dynamic tensile strength, Sandstone, Emulsion explosive, Free surface velocity, High speed photography

## 1. Introduction

The dynamic tensile strength of brittle materials such as rock has been studied by many researchers by using impact tests or explosive loading<sup>1)-7)</sup>. Hino is pioneer who employed the Hopkinson's effect and explosive to estimate the dynamic tensile strength of rock<sup>8), 9)</sup>. He measured the velocity of the fragments of the square stick under explosive loading and determined the shape of the compression wave near the free end to estimate dynamic tensile strength. Ma et al<sup>10)</sup> continually measured the velocity at the free end by using a laser vibration meter, and obtained the dynamic tensile strength in different types of rocks. They used the cylindrical rock specimen and detonator as shock loading in their test. Jung et al also carried out the same type of experiment for Kimachi sandstone<sup>11)</sup>. We have also proposed the dynamic material test of rock utilizing underwater shock wave and Hopkinson's effect<sup>12), 13)</sup>. One of the aims of this test is to construct the estimation method on the dynamic tensile strength of the rock. To accomplish the purpose, it is important to understand the dynamic behaviors of the rock specimen during this

dynamic material test. In this paper, results of a series of our material tests will be described, and dynamic behavior of the cylindrical rock specimen which is made by Kimachi sandstone will be discussed.

## 2. Experiment and theory

The main part of this dynamic material test consists of three parts, cylindrical rock specimen, PMMA Pipe filled with water and explosive part as shown in Fig. 1. The advantage of proposed test is that the strength of the incident shock wave to the rock specimen could be easily adjusted by simply changing the length of the pipe between explosive and rock specimen. In addition the strength and its distribution of the underwater shock wave could be calculated by fluid dynamic code. From the previous numerical simulations, for example when the pipe length is more than 70 mm, the shock front into the rock specimen almost has the plane geometry. Figure 2 shows the experimental set up for the proposed test. The velocity at free end and the cracks at the side of specimen near the free end were observed by a laser vibration

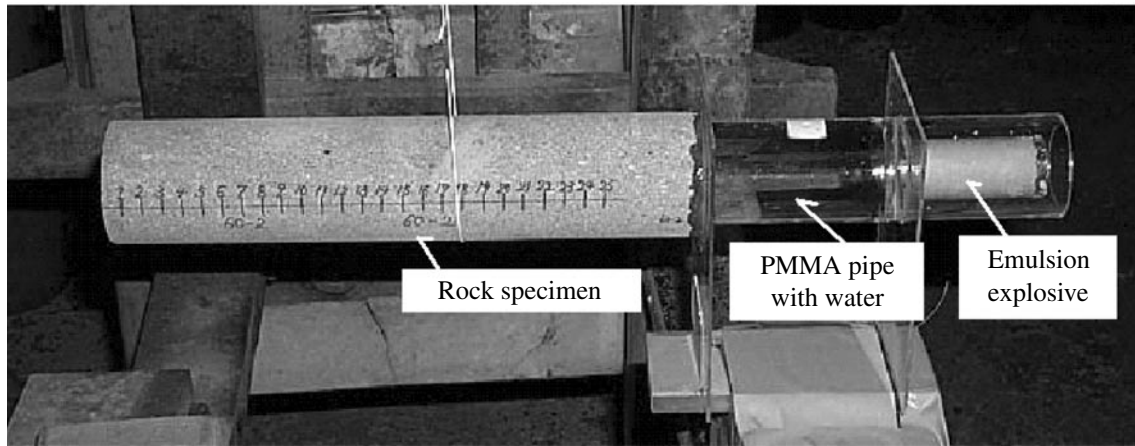


Fig. 1 Main part of proposed dynamic material test. Specimen is Kimachi sandstone with 60 mm diameter and 300 mm length, Explosive is 40 g emulsion explosive.

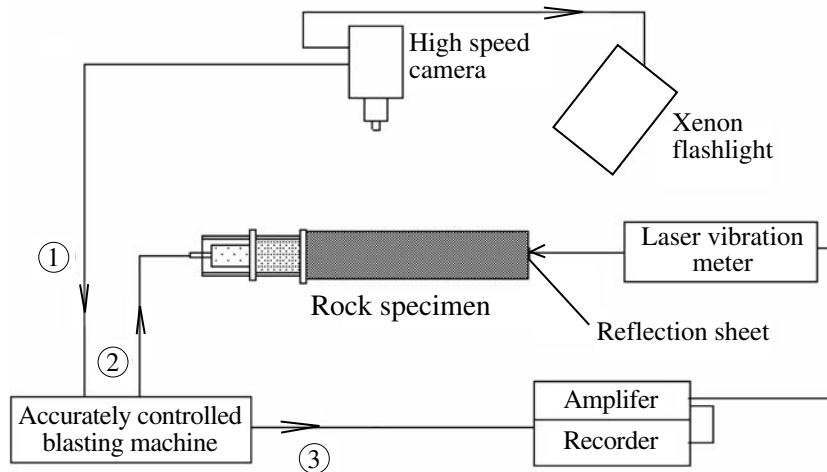


Fig. 2 Whole system of experimental set up. Laser vibration meter (OFV-300; made by Polytec); for Velocity profile at free end, High speed camera (model 124 framing camera; made by Cordin ); for Fracture surface.

meter (OFV-300; made by Polytec) and high speed camera (model 124 framing type camera; made by Cordin) simultaneously. The precise detonator was used to control the initiation time. Emulsion explosive was employed as the explosion source. After the detonation wave interacts with water, the underwater shock wave generates in the water inside the PMMA pipe. The length of the PMMA pipe was varied as 30, 50, 70, 100, 150, 200 and 300 mm. Kimachi sandstone was used as the rock specimen with 60 mm diameter and 300 mm length. The velocity of elastic wave and static tensile strength are measured by ultrasonic and Brazilian tests and are 2742 m s<sup>-1</sup> and 3.7 MPa respectively. The Density of the specimen is 2016 kg m<sup>-3</sup>.

The tensile strength  $\sigma_d$  have been described by,

$$\sigma_d = \frac{\rho C_p}{2} [-v_f(tp + 2\Delta t) + v_f(tp)] \quad (1)$$

Where  $\rho$ ,  $C_p$ ,  $v_f$  and  $\Delta t$  are the density, the velocity of elastic wave, the particle velocity at free surface and  $\delta/C_p$ .  $\delta$  is the distance from the free surface to the fracture surface.  $tp$  is the rise time of compression wave. There are

two assumptions, 1) the phenomenon is one-dimensional, 2) the stress wave is steady near the free surface. In this study this concept has been employed to construct the stress distribution in the specimen.

### 3. Results and discussion

The typical velocity profile at the free end is shown in Fig. 3. The data for three shots are plotted on this figure, and the excellent reproducibility can be confirmed. This high reproducibility on the velocity measurements was confirmed with another pipe length. According to the free surface approximation, stress  $\sigma$  near the free end of the specimen can be written by  $0.5 \rho C_p v(t)$ . Before the stress wave reflects at free end, stress profile near the free end shows the qualitatively same tendency as the velocity profile at free end. After the maximum velocity appears, inflection point, i.e. the local minimum value, appears. It is plausible that this change is caused by drop in strength of the specimen due to crack growth. Therefore after the inflection point, the velocity profile could not be used in the stress wave prediction. The relationship between the

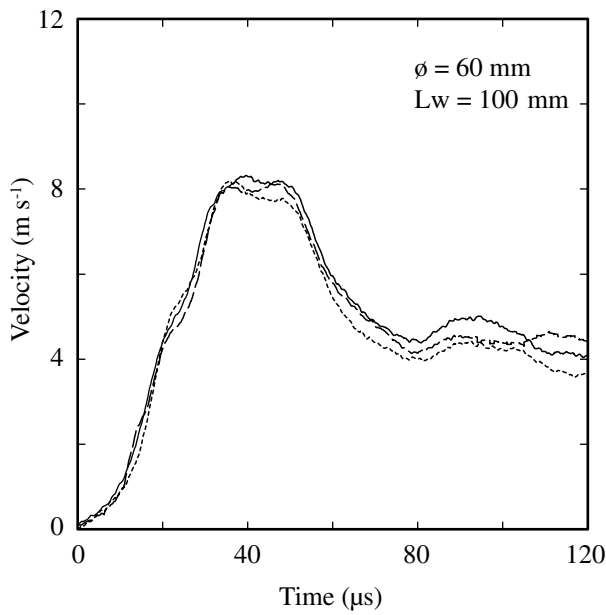


Fig. 3 The velocity profiles at free end of rock specimen under 100 mm pipe.

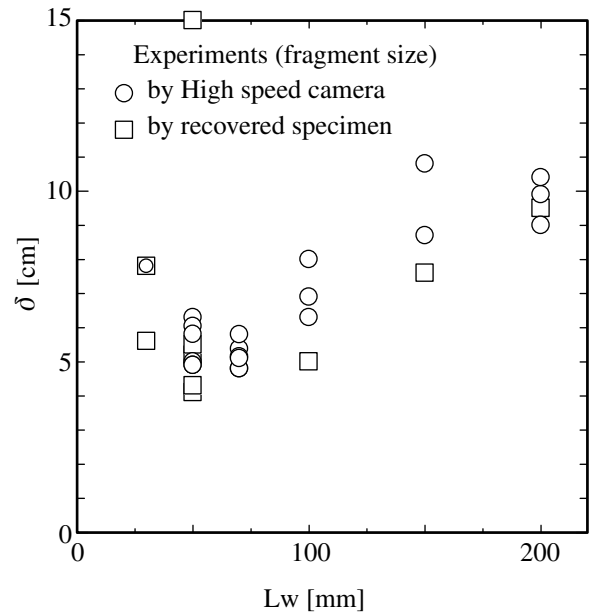


Fig. 4 Pipe length vs. fragment size  $\delta$ . Fragment size means the distance from the free end of the specimen to fracture point where the crack first appeared near the free end.

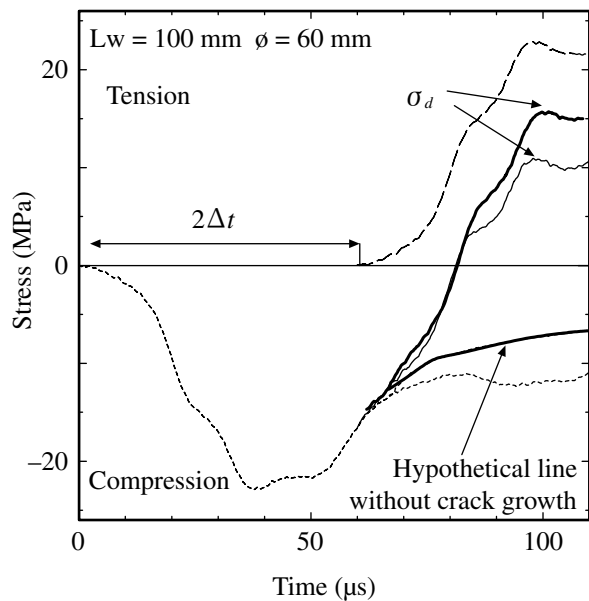


Fig. 5 The stress profile at the fracture surface predicted by velocity profile, Pipe length; 100 mm, Thick solid line corresponds to 'Hypothetical line without information of the crack growth'.

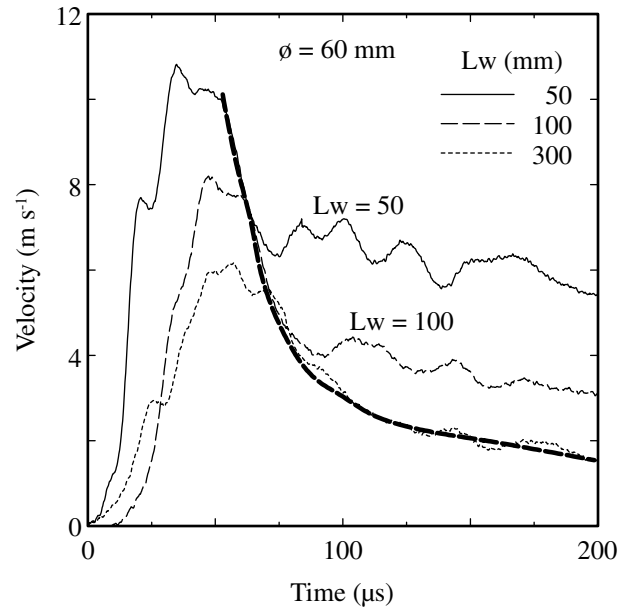


Fig. 6 The velocity profiles at free end for 50, 100 and 300 mm pipe with hypothetical attenuation line (thick dashed line).

pipe length and fragment size,  $\delta$ , that is the distance from the free end of specimen to position where the crack first appeared near the free end is shown in Fig. 4. The fragment size has been mainly measured by high speed photography. The recovery sample was used when the measurement failed. In the case of 300 mm pipe, the fracture cross section could not be measured. It can be seen that when the pipe length is more than 70 mm, the fragment size increases as the pipe length increases. The stress profile at the fracture surface predicted by velocity profile at

free end is shown in Fig. 5 with 'Hypothetical line without information of the crack growth'. If the velocity profile is not modified under reasonable assumption, the dynamic tensile strength is obtained on the thin solid line. Therefore the estimated stress has low value as comparison with real value as shown in Fig. 5. If the cracks do not grow at the intended fracture surface, the velocity profile is smoothly reduced from the maximum value to the minimum. Fortunately in the case of 300 mm pipe the fracture surface was not made by dynamic loading. In such case tendency

of the velocity attenuation include few crack information. The velocity profiles at free end for 50, 100 and 300mm pipe are plotted in Fig. 6 with hypothetical attenuation line. Because the velocity profile can be directly converted to the stress profile, the tendency of the velocity attenuation can be regarded as the tendency of stress attenuation. From Fig. 6 it can be seen that the attenuation processes without the information of the crack initiation or growth have the same attenuation rate each other. Therefore in this experimental result it can be reasonably assumed that regardless of the difference of the dynamic loading, the attenuation rate of stress wave becomes same at any time under the same stress state. Thick solid line in Fig. 6 could be used as attenuation line without crack information. The hypothetical line was used to estimate the stress distribution in this study.

#### 4. Behaviors of cylindrical rock specimen under dynamic load

The propagation processes of tensile wave are shown in Fig. 7 with stress distributions. Time is counted from the compression wave reaches the free end of specimen. The tensile wave propagates from left to right in all figures. Two dotted lines are drawn to indicate the region of fracture cross section, RFCS, which is made by the experimental data in Fig. 4. It can be considered as following. The tensile wave reflected from the free end induces the high stress conditions as compared with the conditions of static. As the results the micro crack in a rock specimen is activated in order to build a damage zone over a certain range. A damage zone is formed first, and a crack grows for producing the fragment. Probably the damage zone will spread out near the fracture cross section. Ai and

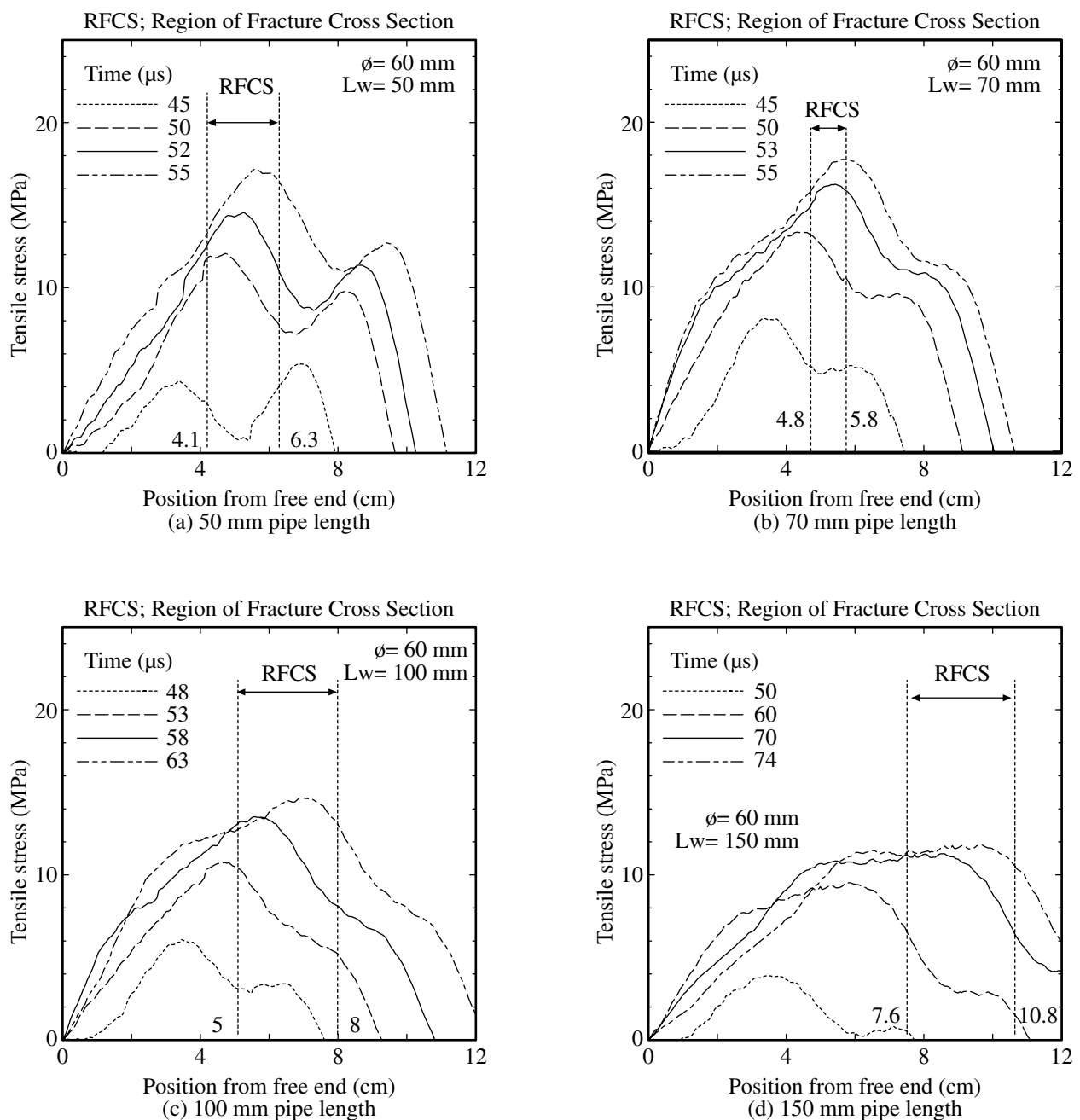


Fig. 7 The propagation processes of tensile wave from the free end of the specimen.  $L_w$ ; pipe length.

Ahrens<sup>5)</sup> have done the impact experiment. They measured the sound velocity of the sandstone in both pre-shot and post shot to estimate the damage of specimen, and determined the onset of tensile fracture based on those data. In the case of 50 mm pipe the distribution of the tensile stress has two local maximum values. While in 70 and 100 mm pipe, the distributions have one distinct local maximum value, and in 150 mm pipe it has relaxed maximum value. In all cases the position of local maximum value, which exceeds at least 10 MPa, is in agreement with the region of fracture cross section. The change rate of maximum value seems to be related to the length of RFCS. In the cases of 50 and 70 mm pipe, there is no remarkable difference in the rising rate. Near the RFCS region, during 2 cm propagation, increase in the maximum value of the tensile stress is about 5 MPa. This rate of stress rise decreases as the pipe length increases. The length of RFCS increases with the rising rate decreases. In 150 mm case, it raises only 1 MPa during 3.2 cm propagation. The rate of stress rise also related to the position of RFCS, i.e. the fragment size. The fragment size increases with the rising rate decreases. Maximum tensile stress values over the region of fracture cross section correspond to the dynamic tensile strength.

## 5. Conclusion

A series of the dynamic test were carried out with various dynamic loading conditions for Kimachi sandstone. Hypothetical release line without fracture information was introduced to predict the complete compression waveform. The relationships of the region or position of fracture surface and the stress distribution have been clearly understood. In the case of 50 mm pipe the distribution of the tensile stress has two local maximum values, while in 70 and 100 mm pipe, the distributions have one distinct local maximum value. This rate of maximum tensile stress

rise decreases with the pipe length increases. The length of RFCS increases with the rising rate decreases. The rate of stress rise also related to the position of RFCS, i.e. the fragment size. The fragment size increases with the rising rate decreases.

## References

- 1) D.E. Grady and R.E. Hollenbach, *Geophys. Res. Lett.*, 6, 2, 73 (1979).
- 2) D.E. Grady and M.E. Kipp, *Int. J. Rock Mech. Min. Sci. & Geomech. Abstr.*, 1, 16, 293 (1979).
- 3) S.N. Cohn and T.J. Ahrens, *J. Geophys. Res.*, 86, B3, 1794 (1981).
- 4) D.D. Shockey, D.R. Curran, L. Seaman, J.T. Rosenberg and C.F. Petersen, *Int. J. Rock Mech. Min. Sci. & Geomech. Abstr.*, 11, 303 (1974).
- 5) H.A. Al and T.J. Ahrens, *Meteorit. Planet. Sci.* 39, Nr2, 233 (2004).
- 6) D.E. Grady and J. Lipkin, *Geophys. Res. Lett.*, 7, 4, 255 (1980).
- 7) S.H. Cho, Y. Ogata, and K. Kaneko, *Int. J. Rock Mech. Min. Sci.*, Vol. 11, pp. 303 (1974).
- 8) K. Hino, *J. the Industrial Explosives Society (Sci. Tech. Energetic Materials)*, 17, 2 (1956).
- 9) K. Hino, *J. the Industrial Explosives Society (Sci. Tech. Energetic Materials)*, 17, 236 (1956).
- 10) G. Ma, A. Miyake, T. Ogawa, Y. Wada, Y. Ogata, M. Seto, and K. Katsuyama, *Kayaku Gakkaishi (Sci. Tech. Energetic Materials)*, 59, 49 (1998).
- 11) W.J. Jung, Y. Ogata, Y. Wada, M. Seto, K. Katsuyama and T. Ogata, *J. of the Japan Society of Civil Engineers*, No.673/III-54, 53 (2001).
- 12) S. Kubota, Y. Ogata, R. Takahira, H. Shimada, K. Matsui and M. Seto, the 4th International Symposium on Impact Engineering, pp. 419-423 (2001).
- 13) S. Kubota, Y. Ogata, WJ Jung, K. Aoki, H. Shimada and K. Matsui, 7th International Symposium on Rock Fragmentation by Blasting, pp. 133-138 (2002).

## 動的荷重下における円筒岩石試料の挙動

久保田士郎<sup>\*\*†</sup>, 緒方雄二<sup>\*</sup>, 和田有司<sup>\*</sup>, シマングソン ガンダ<sup>\*</sup>,  
島田英樹<sup>\*\*</sup>, 松井紀久男<sup>\*\*</sup>

著者らが提案した試験方法によって動的荷重下における岩石試料の挙動が調べられた。試験ではホプキンソン効果を応用した。水で満たされたPMMA製の管が爆薬と岩石試料の間に配置され、PMMA管の長さが動的荷重の大きさを調整するために変化させられた。来待砂岩に対して、一連の動的試験を行った。実験により得られた自由端での速度履歴より、試料中の引張波の伝播過程が求められた。引張波の応力分布から、破断が起る領域と位置と応力分布との関係が明らかになった。

<sup>\*</sup> 産業技術総合研究所 つくば西事業所 〒305-8569 つくば市小野川16-1

<sup>†</sup> Corresponding address: kubota.46@aist.go.jp

<sup>\*\*</sup> 九州大学大学院工学研究院地球資源システム工学専攻 〒812-8581 福岡市東区箱崎6-10-1